ELSEVIER

Journal of Power Sources 115 (2003) 141–148

JOURNAL OF POWER SOURCES

www.elsevier.com/locate/jpowsour

Solar thermolectric generator based on skutterudites

H. Scherrer[a], L. Vikhor[b], B. Lenoir[a,*], A. Dauscher[a], P. Poinas[c]

[a]*Laboratoire de Physique des Matériaux, UMR CNRS-INPL-UHP 7556, Ecole des Mines, Parc de Saurupt, F-54042 Nancy, France*
[b]*Institute of Thermoelectricity, P.O. Box 86, 58002 Chernivtsi, Ukraine*
[c]*ESA ESTEC, P.O. Box 299, 2200AG Noordwijk, The Netherlands*

Received 2 June 2002; received in revised form 5 October 2002; accepted 7 October 2002

Abstract

A numerical simulation based on the optimal control theory was developed to assess the performances, dimensions and weight characteristics of skutterudite-based solar thermoelectric generators (STG) for satellite missions at distances close to the Sun. It is shown that the STG designs based on these advanced thermoelectric materials are potentially attractive for this type of application and could advantageously replace the standard power sources such as the solar (cells) panel or the radioisotope thermoelectric generators.

Keywords: Thermoelectric devices; Thermoelectric energy conversion; Skutterudites; Optimal control theory

1. Introduction

So far, the primary power sources used on unmanned spacecraft applications are the solar arrays and the radioisotope thermoelectric generators (RTG). However, when working at distances close to the Sun, the use of solar cells is limited by two factors: (1) the high incident solar heat flux tends to produce high solar cell temperatures and (2) the high incident radiation flux causes cell damage. Both factors yield rapid deterioration of the solar cell performance. Even if the solar cells are temperature controlled and protected against the radiation damages, they become less attractive in near-Sun missions because of increased weight and decreased reliability. RTG have been extensively used on interplanetary US satellites, but are not used since more than 10 years on board European scientific satellites. The environmental risks in case of explosion during the ascent and the difficulty to import such system were the main reasons to abandon this technology.

Among candidates other than RTG that could operate efficiently and power satellites flying near to the Sun, the solar thermoelectric generators (STG) could be an interesting alternative solution, because the thermoelectric materials are in general less sensitive to both the temperature and the radiation damages. Systems based on STG have already been described in the past [1–7].

A complete STG consists of the collector/concentrator, the thermopiles, the insulation and the radiator. The material selection for each of these four parts is of the greatest importance in the overall performance and weight characteristics of the system and shall be considered in details. Referring to the approximate relation:

$$\eta \approx \tfrac{1}{4} Z\Delta T \qquad (1)$$

it is easily seen that in order to achieve a high efficiency η, the temperature difference ΔT across the thermopile should be as high as possible, and the thermocouples constituting the thermopile should possess a high figure-of-merit Z. Because Z of established thermoelectric materials differ, as do the ranges of temperature difference across which they can be operated, it is normally found that most thermoelectric materials yield performance values that differ somewhat from each other. Over the past few years, much effort has been devoted to achieve high Z values through the exploration of new classes of materials such as semiconductors and semimetals with complex open crystal structures allowing for very low thermal conductivity [8,9]. Among them, skutterudites based on $CoSb_3$ have been recently promoted as possible new thermoelectric materials [8–10]. n- and p-type materials have been synthesized and were found to have higher figure-of-merits than those of the established Si–Ge based alloys in the temperature range 300–1000 K.

In order to assess the performance, dimensions and weight characteristics of a skutterudite-based STG for near-Sun missions, a physical model has to be developed. The number

* Corresponding author. Tel.: +33-3-83-58-41-63;
fax: +33-3-83-57-97-94.
E-mail address: bertrand.lenoir@mines.inpl-nancy.fr (B. Lenoir).

0378-7753/02/$ – see front matter
PII: S0378-7753(02)00597-9

of variables is important and it is necessary to solve a number of optimizing problems. The algorithm for the optimization was generally based on classical energy balance equations, which did not take into account neither the dependences of the thermoelectric parameters on the temperature, nor the contact resistances which may result in great errors [1,6]. The above-mentioned approximations can be avoided using modern methods of optimization, for instance the optimal control theory [11,12].

In this paper, we present a numerical simulation using the optimal control theory to design a STG based on skutterudite thermoelectric materials. In a first place, the mathematical development is presented. It is then used to study parametrically the performance and the mass analysis of three different STG concepts. These results are discussed in details in relation with the STG design. The imposed requirements for the STG were: (i) the orientation perpendicular to the Sun, (ii) the production of 400 W electrical power and (iii) the working distance of 0.45 a.u. from the Sun that corresponds to Mercury (average).

2. Design method of STG

2.1. Physical model for STG

A complete STG consists of a solar concentrator or collector, a set of thermopile units, insulating parts and a radiator (Fig. 1a). Several types of concentrators can be used for increasing the solar intensity and acquiring an increase in thermal flux on the hot junction surface of the thermopiles. The configurations of interest discussed in earlier papers involve a flat-plate collector [1–3] or a compact design with a single concentrator or with multiple solar mini-concentrators [4,5]. A single thermopile consists of several thermoelectric couples (n- and p-type), connected usually in series, sandwiched between two ceramic plates and sealed around the edges (Fig. 1b). This structure allows to connect the thermopiles in parallel within the STG providing more reliable operation of the thermoelectric device as a whole. The space between the collector and radiator plates not occupied by the thermopiles is filled with a thermal insulator to reduce the shunt heat losses.

The schematic diagram of a flat-plate STG, shown in Fig. 1, is used to establish the appropriate mathematical relationships of the STG physical model. For simplicity, the heat flow is assumed to be one-dimensional. This assumption is reasonable, since the collector and radiator plates are usually thin and made of materials with good thermal conductivity. Therefore, the heat flow along the STG due to local temperature gradients is neglected as it is usually compared to the heat flux across the STG. The heat losses from the edges of the insulator, collector and radiator plates are neglected.

The collector plate is assumed to be exposed to a perpendicular solar flux. The heat absorbed, Q_a, is basically dependent on the distance from the Sun d and can be determined as follows:

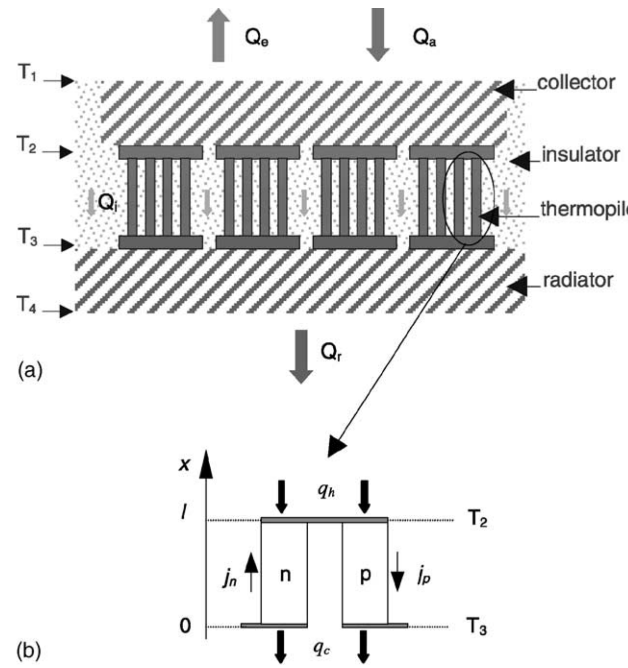

Fig. 1. (a) The principle scheme of a flat-plate STG. (b) Schematic diagram of a single thermoelectric couple constituted of n-and p-type semiconducting branches.

$$Q_a = \frac{\alpha_a S_c}{d^2} A_1 \quad (2)$$

where α_a is the absorptivity of the collector coating, S_c the solar constant at 1 a.u. in space ($S_c = 1370$ W/m^2) and A_1, the collector area. The amount of heat Q_e re-radiated from the collector surface into space at 0 K (assumed temperature) is given by:

$$Q_e = \varepsilon_1 \sigma_{SB} A_1 T_1^4 \quad (3)$$

where ε_1 is the emissivity of the collector coating, σ_{SB} the Stefan-Boltzmann constant and T_1 the temperature of the collector surface.

The shadow face, i.e. the radiator, is cooled by the radiation of heat flowed through the thermopiles and the insulation to deep space. This amount of heat, Q_r, lost into space is given by:

$$Q_r = \varepsilon_2 \sigma_{SB} A_2 T_4^4 \quad (4)$$

where ε_2 is the emissivity of the radiator coating and A_2, T_4 the area and the temperature surface of the radiator, respectively.

In operation, the total heat transported through the STG is the amount of heat absorbed by the collector from the Sun minus the energy converted to electric power.

Written in terms of heat flux densities for steady-state conditions, the previous energy balance equations become:

$$q_a - q_e = \frac{1}{R_1 h_1}(T_1 - T_2) \quad (5)$$

$$q_r = \frac{1}{R_2 h_2}(T_3 - T_4) \quad (6)$$

$$q_aK_1 - q_eK_1 - q_h(T_2, T_3) - q_i(K_2 - 1) = 0 \quad (7)$$

$$q_rK_2 - q_i(K_2 - 1) - q_c(T_2, T_3) = 0 \quad (8)$$

where R_1 and R_2 are the specific heat resistances of collector and radiator materials, h_1, h_2 the thicknesses of these materials, $K_1 = (A_1/A_{TE})$, $K_2 = (A_2/A_{TE})$ the ratios of collector A_1 and radiator A_2 areas to the thermopiles area A_{TE}.

In the set of Eq. (5)–(8), q_a represents the density of heat absorbed by the collector from the Sun:

$$q_a = \frac{Q_a}{A_1} = \frac{\alpha_a S_c}{d^2} \quad (9)$$

q_e denotes the density of heat re-radiated by the collector surface:

$$q_e = \frac{Q_e}{A_1} = \varepsilon_1 \sigma_{SB} T_1^4 \quad (10)$$

q_r, is the density of heat emitted by the radiator surface:

$$q_r = \frac{Q_r}{A_2} = \varepsilon_2 \sigma_{SB} T_4^4 \quad (11)$$

and q_i is the density of heat transported through the insulation:

$$q_i = \frac{Q_i}{A_2 - A_{TE}} = \frac{\lambda}{h_i}(T_2 - T_3) \quad (12)$$

where λ is the thermal conductivity of the insulator and h_i the thickness of insulation between the collector and the radiator.

The densities of heat absorbed at the hot junctions of the thermocouples and rejected at the cold thermoelectric junctions are denoted as q_h, q_c, respectively. These two heat flux densities depend on the temperatures of hot T_2 and cold T_3 sides of the thermopiles (see Fig. 1). They are also assigned by the operating mode of the thermocouples. Expressions (5)–(8) with the additional relationships for calculation of heat densities q_h and q_c form a system of four nonlinear equations which for any couple of given K_1 and K_2 values define uniquely the unknown temperatures T_1, T_2, T_3, T_4. Using these data, all unknown characteristics of the STG can be estimated.

The relationships for heat densities q_h and q_c can be obtained from the theory of thermoelectric conversion, using the detailed optimization of thermoelectric device performance.

2.2. Design optimization of thermoelectric devices

Several methods have been used for designing and optimizing thermoelectric power generators with solar heat source [1,2,6,7]. The main imperfection arises from the fact that most of them are based on the relationships of heat balance at the hot and the cold junctions of the thermoelements which are only valid when Joule and Thomson heats are small in comparison to the conduction heat and when electrical resistivity, thermal conductivity, and Thomson coefficient are not temperature dependent. In most of the earlier published papers, Thomson heat is even neglected [1,6]. This approach is appropriate only for materials with little variation of the Seebeck coefficient with temperature. But in the case of thermoelectric generation under large temperature gradients, the dependence of the material parameters on temperature is appreciable and should be taken into account. Moreover, some important factors such as thermal and electrical contact resistances are not always considered. It is often assumed that thermocouples have a fixed configuration and optimization is made by calculation of the device performance for combination of values for some variables [2,3]. In such methods the number of combinations is limited, which may lead to inaccurate optimization results.

More recently, a novel numerical method suitable for computer implementation has been developed for design and optimization of performance of thermoelectric systems. It enables to overcome the shortcomings of the previous methods. This numerical simulation, based on the mathematical theory of optimal control [11,12] is very attractive for the optimization and the prediction of the thermoelectric module performance. It has been developed in details for thermoelectric coolers and has been further extended successfully to optimize thermoelectric generators [13,14]. We propose here to apply this method to extract the heat flux densities q_h and q_c at the hot and cold junctions of the thermopiles (T_2 and T_3) involved in the system of balance Eqs. (5)–(8).

The initial data for the STG design are the output electrical power W_L and voltage V_L on the external load. It is also important to select the mode of operation of the generator. For this purpose, the STG efficiency can be written as follows:

$$\eta_{STG} = \frac{W_L}{Q_a} = \frac{w}{q_aK_1} \quad (13)$$

where $w = (W_L/A_{TE})$ is the output electric power per unit of thermoelement area.

In our case the solar heat density q_a is fixed. Therefore, for any given K_1 value, the maximum STG efficiency mode is equivalent to the maximum output power density w, which is:

$$w = q_h - q_c \quad (14)$$

The problem is then to maximize the functional w.

Temperature $T(x)$ and heat flux $q(x)$ distributions within one of the legs (n or p) of a thermocouple at a distance x from the cold junction (Fig. 1) are determined by the system of four differential equations of the form [13]:

$$\left.\begin{aligned} \frac{dT}{dx} &= -\frac{\alpha j}{\kappa}T - \frac{q}{\kappa} \\ \frac{dq}{dx} &= \frac{\alpha^2 j^2}{\kappa}T + \frac{\alpha j}{\kappa}q + \frac{j^2}{\sigma} \end{aligned}\right\}_{n,p} \quad (15)$$

where α, σ, κ are the Seebeck coefficient, the electrical conductivity and the thermal conductivity, respectively and j the current density.

In this system, the thermoelectric material properties $\alpha(T)$, $\sigma(T)$, $\kappa(T)$ are temperature dependent and, approximated by polynomials. The solution of Eq. (15) under the following boundary conditions:

$$T_n(0) = T_p(0) = T_3, \quad T_n(l) = T_p(l) = T_2 \tag{16}$$

gives the opportunity to calculate the heat flux densities at the hot and cold thermoelements junctions q_h and q_c using the expressions:

$$\begin{aligned} q_h &= -\sum_{n,p}[q(l) + j^2 r_c] \\ q_c &= -\sum_{n,p}[q(0) - j^2 r_c] \end{aligned} \tag{17}$$

where r_c is the contact resistance and l the thermoelement legs height.

The relation (17) shows that q_c and q_h depend on the current densities $j_{n,p}$. These parameters have to be evaluated in order to maximize the functional w.

The optimal control method allows to make a purposeful search for $j_{n,p}$ values [11,13]. According to this method, optimal current densities should satisfy the following relationships:

$$-\frac{\partial w}{\partial j_{n,p}} + \int_0^l \frac{\partial H(\psi, T, q, j_n, j_p)}{\partial j_{n,p}}\,dx = 0,, \tag{18}$$

where the Hamilton function H has the form:

$$H = \sum_{n,p}(\psi_1 f_1 + \psi_2 f_2) \tag{19}$$

where $(f_1, f_2)_{n,p}$ are the right parts of (15) and $\psi = (\psi_1, \psi_2)_{n,p}$ is the pulse vector conjugated to the phase variable vector $y = (T, q)_{n,p}$. Its determination is detailed elsewhere [13].

The numerical method of successive approximations can be recommended to solve this optimal control problem. It allows to calculate the optimal current densities $j_{n,p}$ and heat fluxes q_h, q_c values respective to the maximum w.

2.3. Computer algorithm for the STG design

The algorithm of the STG design method described above is based on the numerical solution of the heat balance system (5)–(8) relative to the unknown temperatures $T_1, \ldots, T_4$ for given factors K_1 and K_2. The method of Newton's iterations has been used for solving the nonlinear equations system. A subroutine was used to calculate the optimal heat densities q_h and q_c. It should be noted that the equation system (5)–(8) includes only two independent nonlinear Eqs. (7) and (8) with respect to the independent variables T_1, T_4. The temperatures T_2, T_3 are defined in Eqs. (5) and (6).

For such a calculation, an initial value must be given to all materials properties as well as the length of the thermoelement legs. The result of the calculation gives a complete spectrum of temperatures $T_1, \ldots, T_4$ and correspondent values of maximum output power density w, optimal heat fluxes q_h, q_c, and current densities j_n, j_p. Then, for the required power W_L and voltage V_L on the external load, the complete performance and parameters of the STG structure can be estimated using the following relationships:

The thermoelectric generator efficiency η:

$$\eta = \frac{w}{q_h} = \frac{q_h - q_c}{q_h} \tag{20}$$

The thermopiles area:

$$A_{TE} = \frac{W_L}{w} = \frac{W_L}{q_h - q_c} \tag{21}$$

The collector surface area A_1 and the radiator surface area A_2:

$$A_1 = K_1 A_{TE}, \quad A_2 = K_2 A_{TE} \tag{22}$$

The heat fluxes through the collector plate Q_s and radiator plate Q_r:

$$Q_s = A_1(q_a - q_e), \quad Q_r = A_2 q_r, \tag{23}$$

The single thermopile area (for a given number of thermopiles N):

$$A = \frac{A_{TE}}{N} \tag{24}$$

The single thermopile electric power W, voltage V and current I:

$$W = \frac{W_L}{N} \tag{25}$$

$$V = \frac{V_L}{N} \quad \text{(for series thermopile connection)}, \tag{26}$$

$$V = V_L \quad \text{(for parallel connection)}, \tag{27}$$

$$I = \frac{W}{V} \tag{28}$$

The cross-sections of n- and p-type legs $A_{n,p}$:

$$A_{n,p} = \frac{I}{j_{n,p}} \tag{29}$$

The number of thermocouples connected in series per thermopile N_{TE}:

$$N_{TE} = \frac{A}{(A_n + A_p)} \tag{30}$$

The weight of the STG can be directly calculated from the dimensions and the material characteristics used for the collector, the radiator, the insulation and the thermopiles.

As a result, the optimal STG performance in maximum conversion efficiency mode and simultaneously in maximum power output per unit surface of thermoelectric device mode are known for any given factor K_1 and K_2. The optimization of the performance with respect to K_1 and K_2 should be made through the variation of these parameters.

Based on this algorithm, a computer program for STG design has been developed.

2.4. STG concepts and material selection

The proposed mathematical model has been successfully used for the design of three STG concepts with regard to factors K_1 and K_2. In the first concept, collector and radiator plates are assumed to have identical areas ($K_1 = K_2$). It is a so-called flat-plate STG (Fig. 1). The second one is a STG having the radiator plate area larger than the collector plate area ($K_2 > K_1$). The third concept is concerned with a STG configuration with a single solar concentrator or with mini-solar concentrators for each thermopile unit, in place of the flat-plate collector. This configuration is exemplified in Fig. 2. In this case K_1 is interpreted as a concentration ratio (usually $K_1 > K_2$). The advantages of one STG concept on another can only be estimated on the basis of the calculation results.

The evaluation of the performance and weight characteristics of the three STG designs has been accomplished for a 0.45 a.u. operation distance, a 400 W load and according to the following material selection. As previously stated, we propose to use skutterudite materials as thermoelectrics. This novel family of materials has received considerable attention this last decade and continues to be extensively investigated due to their unique electrical and thermal properties. Their use in thermoelectric devices for terrestrial or space power generations has also been considered and the results seem to be very promising [15]. Among skutterudite materials, filled $CoSb_3$ (*p*-type) and doped $CoSb_3$ (n-type) are known to possess high thermoelectric performance in the temperature range 400–1000 K making them very attractive for STG applications. The density of these materials, relatively low, is near 7.65 g/cm^3.

The choice of the collector and radiator materials was principally guided by two rules: a high thermal conductivity and a low weight, compatible with the spacecraft technology. For the calculations, we tentatively selected collector and radiator of aluminum nitride (AlN) that has a thermal conductivity of about 100 W/mK at high temperature and a density of about 3.3 g/cm^3. It is assumed that the collector is covered with a particular coating ensuring high solar absorptance and low emittance (collector absorptivity $\alpha_a = 0.9$; collector emissivity $\varepsilon_1 = 0.08$). Conversely, the radiator is covered with an optical coating ensuring high heat rejection (radiator emissivity $\varepsilon_2 = 0.75$).

The material ensuring the thermal insulation between the collector and the radiator plates must have a thermal conductivity as low as possible in order to reduce shunt heat transfer. Our calculations were performed assuming the use of a thermal insulator from Microtherm Society, having a thermal conductivity of 0.035 W/mK within the operating temperature range and a density of 0.24 g/cm^3. This insulator is located between the individual thermopiles within the STG, so that the minimum height of insulation to consider is the height of the thermopile. Vacuum is assumed to be in-between the legs of the thermopile. The value of the contact resistance between the cold and hot electrodes and the legs of the thermoelements was assumed to be equal to $5 \times 10^{-6}\ \Omega\,cm^2$.

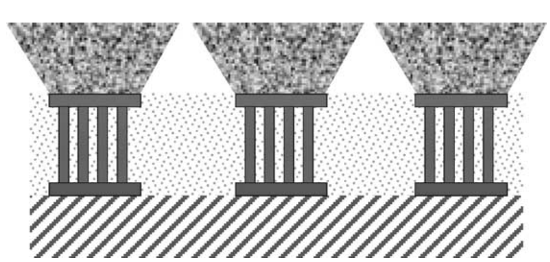

Fig. 2. Schematic diagram of a STG with multiple solar concentrators.

3. Results and discussion

The next paragraphs present the results obtained from the numerical simulation for the three STG concepts. The analysis focuses on the influence of K_1 and K_2 values on the dimensions, performances and weight characteristics of the STG. The complete description of the system will not be described here, as for instance the number of thermocouples per thermopile, the cross-section of the n- and p-legs and the current used. These data can be estimated in a straightforward way once N and V are fixed using the set of Eqs. (24)–(30) exposed in Section 1.3.

3.1. Concept I: collector and radiator of same area

The first calculations have been carried out for a flat-plate STG model with collector and radiator of equal area A. The modeling results obtained for thermoelectric legs of 1 cm in height, an insulation thickness of 1.5 cm and plates of collector and radiator of 1 mm in thickness are summarized in Table 1. The temperature drops ΔT between the collector and the radiator surfaces (T_1–T_4), as well as between the hot side and the cold side of the thermopile surfaces (T_2–T_3), the efficiency η, the collector and radiator area A, the total area of the thermopiles A_{TE}, the mass of thermoelectric material M_{TE}, the overall STG mass M_F, the heat fluxes through the collector Q_s and the radiator Q_r, the specific power W/M_F, the power per unit area W/A_2 are reported for various values of ratio K (A/A_{TE}).

Taking into account the dimension parameter, the results indicate that there is an optimum value of K to get the lowest area A. The minimal area A is 2.4 m^2 matching K ratio values between 35 and 40. Under these optimal conditions, the power per surface unit reaches 167 W/m^2 and the tempera-

Table 1
Modeling results for a STG designed according to concept I (flat-plate), for different $K = A/A_{TE}$ values (output power: 400 W, working distance: 0.45 a.u., thermoelectric legs length: 1 cm, insulating thickness: 1.5 cm, radiator and collector plate thickness: 0.1 cm, materials and properties as defined in the text)

K	T_1–T_4, T_2–T_3 (K)	η (%)	A (m^2)	A_{TE} (m^2)	M_{TE} (kg)	M_F (kg)	Q_s (kW)	Q_r (kW)	W/M_F (W/kg)	W/A_2 (W/m^2)
20	779.3–562.8, 779.2–562.9	3.8	2.64	0.132	10.13	36.4	11.70	11.30	11.0	151
25	802.9–555.3, 802.8–555.4	4.4	2.50	0.100	7.63	32.5	10.49	10.09	12.3	160
30	822.1–548.6, 822.0–548.7	4.9	2.43	0.081	6.18	30.4	9.73	9.33	13.2	165
35	838.1–542.5, 838.0–542.6	5.2	2.38	0.068	5.24	29.2	9.23	8.83	13.7	167
40	851.6–537.0, 851.5–537.1	5.6	2.40	0.060	4.59	28.6	8.88	8.48	14.0	167
45	863.1–532.0, 863.0–532.1	5.9	2.43	0.054	4.11	28.4	8.64	8.24	14.1	165
50	873.0–527.4, 873.0–527.5	6.1	2.45	0.049	3.75	28.4	8.47	8.07	14.1	163
55	881.7–523.2, 881.6–523.3	6.3	2.48	0.045	3.47	28.5	8.35	7.95	14.0	160
60	889.3–519.4, 889.3–519.4	6.5	2.52	0.042	3.24	28.8	8.27	7.87	13.9	158

ture difference is about 310 K. A relatively high efficiency of about 5.5% is achieved with a low amount of thermoelectric material (near 5 kg). The overall STG mass includes the thermoelectric material mass, the insulator mass, which is about 8.5 kg in this case, and the collector and radiator masses. The latter depend of course on the AlN plate thickness of the collector and radiator. The influence of the thickness (varied between 2.5 and 0.63 mm) on the key parameters has been investigated. It is found that the results have little effect except on the overall weight of the STG as illustrated in Fig. 3 for the best configuration. For a thickness of 1 mm, the weight of the STG is near 29 kg but can be reduced down to 23 kg by decreasing the plate thickness to 0.63 mm.

Hot and cold side temperatures ranging between about 780–890 and 520–560 K, respectively, are well in the range of the operating temperature of skutterudite materials. It has to be noted that the temperature drops through the collector and radiator plates are less than 0.1 K and can be therefore neglected.

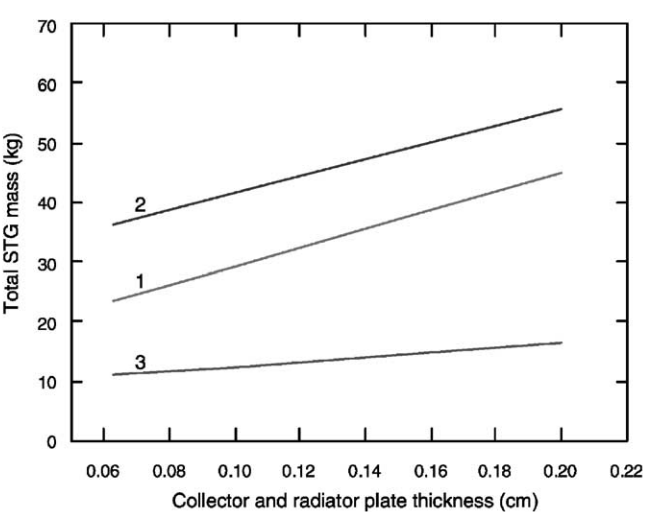

Fig. 3. Dependence of the overall STG mass on the thickness of the radiator and collector plate for various STG concepts delivering 400 W at a working distance of 0.45 a.u. 1: Design I, $l = 1$ cm, $K = A/A_{TE} = 35$; 2: design I, $l = 2$ cm, $K = A/A_{TE} = 22$; 3: design III, $l = 1$ cm, $K_1 = 55$, $K_2 = A_2/A_{TE} = 25$ (total mass is shown without mass of concentrator (no collector plate)).

It is necessary to note that the STG efficiency can be enhanced by increasing the K ratio mainly because of an enhancement of the temperature gradient across the thermopiles. This ratio must, however, not exceed too large values (50 is a limit), otherwise the transverse heat flows due to the temperature distribution along the collector and radiator surfaces will be considerable, resulting in a significant deterioration of the STG performance. Therefore, the results for K values greater than 50 should not be considered.

Similar calculations have been carried out for thermoelectric legs of 2 cm in height (instead of 1 cm) coupled to an insulation 2.5 cm thick. The associated dimensions and performance resulting from this study are summarized in Table 2. In this case, the minimal STG area is even smaller than in the previous case because the heat losses through the insulating parts decrease due to its greater thickness. It is equal to 2.16 m^2 at optimal ratio $K = 20$. It is also accompanied by an enhancement of the power per surface unit up to 185 W/m^2, for a temperature difference of 330 K and with an efficiency that reaches 5.9%. But consequently the mass of required thermoelectric material rises up to 15 kg and full STG mass will also be significantly greater (about 43 kg). The overall STG mass is, as in the previous case, dependent on AlN plate thickness (Fig. 3).

As it was demonstrated previously, the influence of the length of the skutterudite thermoelement is crucial for the results. Decreasing the height implicitly means a decrease of the cross-section, to keep their ratio equal to its optimal value, and so a lesser soldered junction area. It is clear that a strong reduction of these surfaces is not favorable to the mechanical strength of the thermopile since it will affect the durability of the STG structure. For these practical reasons, investigation for leg length less than 1 cm was not considered.

3.2. Concept II: larger radiator than collector area

This second design is derived from the first configuration. It consists of a larger radiator than collector area (Fig. 1). This configuration has retained our attention because by enhancing the radiator area relative to the collector area, one can hope to shift the cold temperature towards lower values

Table 2
Modeling results for a STG designed according to concept I (flat-plate), for different $K = A/A_{TE}$ values (output power: 400 W, working distance: 0.45 a.u., thermoelectric legs length: 2 cm, insulating thickness: 2.5 cm, radiator and collector plate thickness: 0.1 cm, materials and properties as defined in the text)

K	T_1–T_4, T_2–T_3 (K)	η (%)	A (m^2)	A_{TE} (m^2)	M_{TE} (kg)	M_F (kg)	Q_s (kW)	Q_r (kW)	W/M_F (W/kg)	W/A_2 (W/m^2)
16	837.2–542.3, 837.1–542.4	5.2	2.19	0.137	21.0	47.5	8.46	8.06	8.41	182
18	850.2–537.0, 850.1–537.0	5.6	2.17	0.121	18.4	44.9	8.07	7.67	8.92	184
20	861.5–532.0, 861.4–532.1	5.9	2.16	0.108	16.6	42.9	7.77	7.37	9.32	185
22	871.4–527.3, 871.4–527.4	6.1	2.17	0.099	15.1	41.6	7.53	7.13	9.61	184
24	880.3–523.0, 880.2–523.1	6.3	2.18	0.091	13.9	40.7	7.35	6.95	9.84	183
26	888.3–518.9, 888.2–519.0	6.7	2.21	0.085	13.0	40.0	7.20	6.80	10.0	181
28	895.4–515.1, 895.3–515.2	6.7	2.24	0.080	12.2	39.6	7.07	6.67	10.1	179
30	901.9–511.5, 901.8–511.6	6.9	2.25	0.075	11.5	39.3	6.98	6.58	10.2	177

resulting in higher performance. Actually, preliminary results assuming perfect insulating parts suggested that this configuration could be very promising.

The calculations have been made for various ratios of collector to thermopiles areas K_1 and radiator to thermopiles areas K_2 assuming a thermoelement length of 1 cm. It has been further assumed, for simplicity, that the surface of the insulating parts facing the Sun has the same temperature as the collector. The results are reported in Table 3 for the particular case $K_1 = 20$. The data clearly show that the increase of K_2 leads only to an increase of the STG dimensions and mass, and also to bad performances (low temperature difference: ~225 K, low efficiency: ~3.8%). These conclusions remain valid when increasing K_1. The reason is that an increase of the radiator area respective to the collector results in an increase of the shunt heat transported through the insulation. Then, the amount of heat dissipated by the radiator is enhanced, restraining the STG performances. Thus, compared to the ideal case (presence of a perfect insulator) the real case is less attractive and this concept may be discarded.

3.3. Concept III: collector made of multiple mini-concentrators

The last concept considered is based on the use of solar concentrators. There are several types of concentrators that could be used, but their description is outside the scope of this paper (see an example in Fig. 2). The results of the simulation for this configuration are reported in Table 4 for the case $K_2 = 25$. It can be seen that a significant decrease of the STG area can be obtained by increasing the solar concentration coefficient K_1. For similar efficiency and temperature difference the radiator area is decreased by 60% as compared to a flat-plate STG (design I), resulting in high power per unit surface. It is clear that the total mass of radiator, insulator and thermopiles will also be reduced (note that M_F does not take into account the mass of the solar concentrator). This mass reduction, illustrated in Fig. 3, contributes directly to a high specific power. But it must be kept in mind that the increase of the solar concentration coefficient shifts the hot side temperature towards the upper level and therefore care has to be taken not to exceed the operating temperature range of the thermoelectric materials. It is apparent from these results that the dimensions and performance of this STG concept using solar concentrators are very attractive but from a practical point of view the technical development of such configurations seems to be more complex as compared to that of a flat-plate STG.

4. Conclusion

A theoretical simulation of the performances, dimensions and weight characteristics of STG has been presented. As active materials, we used the potential of advanced thermoelectric materials based on skutterudites. The analysis of three STG designs has been carried out for operation at a distance of 0.45 a.u. from the Sun and for 400 W requirements. Through this exploratory work, it is shown that an STG based on the use of skutterudite thermoelectric materials offer attractive performance features as primary or auxiliary power source for spacecraft in near-Sun missions. The skutterudite materials are however still under development and need to be fully characterized in terms of performance and long life operation.

Table 3
Modeling results for a STG designed according to concept II (flat-plate), for $K_1 = A_1/A_{TE} = 20$ and different $K_2 = A_2/A_{TE}$ values (output power: 400 W, working distance: 0.45 a.u., thermoelectric legs length: 1 cm, insulating thickness: 1.5 cm, radiator and collector plate thickness: 0.1 cm, materials and properties as defined in the text)

K_2	T_1–T_4, T_2–T_3 (K)	η (%)	A_1 (m^2)	A_2 (m^2)	A_{TE} (m^2)	M_{TE} (kg)	M_F (kg)	Q_s (kW)	Q_r (kW)	W/M_F (W/kg)	W/A_2 (W/m^2)
20	779.3–562.8, 779.2–562.9	3.8	2.64	2.65	0.132	10.1	36.4	11.7	11.3	11.0	151
30	742.1–517.1, 742.0–517.1	3.9	2.60	3.90	0.130	9.96	44.7	12.3	11.9	8.95	102
40	713.0–486.6, 712.9–486.6	3.8	2.68	5.37	0.134	10.3	55.3	13.2	12.8	7.23	74
50	688.4–464.0, 688.3–464.1	3.7	2.82	7.07	0.141	10.8	68.0	14.3	13.9	5.88	56

Table 4
Modeling results for a STG designed according to concept III (solar concentrator), for $K_2 = A_2/A_{TE} = 25$ and different K_1 values being here the concentration coefficients (output power: 400 W, working distance: 0.45 a.u., thermoelectric legs length: 1 cm, insulating thickness: 1.5 cm, radiator plate thickness: 0.1 cm, materials and properties as defined in the text)

K_1	T_1–T_4, T_2–T_3 (K)	η (%)	A_2 (m^2)	A_{TE} (m^2)	M_{TE} (kg)	M_F[a] (kg)	Q_s (kW)	Q_r (kW)	W/M_F[a] (W/kg)	W/A_2 (W/m^2)
30	835.9–568.9, 835.8–569.0	4.8	2.07	0.083	6.31	20.1	9.59	9.19	19.9	194
40	882.7–588.1, 882.6–588.2	5.3	1.60	0.064	4.90	15.6	8.54	8.14	25.6	250
45	899.8–595.2, 899.7–595.3	5.5	1.47	0.059	4.48	14.3	8.21	7.81	28.0	273
50	914.1–601.1, 914.0–601.2	5.7	1.35	0.054	4.17	13.3	7.96	7.56	30.1	294
55	926.2–606.1, 926.1–606.3	5.9	1.28	0.051	3.92	12.5	7.75	7.35	32.0	312

[a] Without mass of concentrator.

Acknowledgements

This work was supported by ESTEC/ESA, contract No. 15071/01/NL/PA.

References

[1] N. Fuschillo, R. Gibson, F.K. Eggleston, J. Epstein, Adv. Energy Conversion 6 (1966) 103.
[2] V. Raag, Energy Conversion 8 (1968) 169.
[3] V. Raag, R.E. Berlin, Energy Conversion 8 (1968) 161.
[4] V. Raag, L. Hankins, M. Swerdling, in: Proceedings of the 2nd International Conference on Thermoelectric Energy Conversion, Arlington, 1978, p. 60.
[5] V. Raag, L. Hankins, M. Swerdling, R. Ivanoff, Proceedings of the 13th IECEC, San Diego, 1978, p. 1699.
[6] P.S. Castro, W.W. Happ, J. Appl. Phys. 31 (1960) 1314.
[7] A.S. Ohotin, A.A. Efremov, V.S. Ohotin, A.S. Pushkarskii, Thermoelectric Generators, Atomizdat, Moskow, 1971, p. 288 (in Russian).
[8] A. Dauscher, B. Lenoir, H. Scherrer, T. Caillat, Recent Research Development in Material Science, Sign Post, in press.
[9] G.S. Nolas, J.W. Sharp, J.H. Goldsmid, Thermoelectrics: Basic Principles and New materials Developments, Springer, Heidelberg, 2001.
[10] C. Uher, Semicond. Semimetals 69 (2001) 139.
[11] A. Braison, Ho U-Shi, Applied Theory of Optimal Control, Mir, Moskow, 1972, p. 544.
[12] L.S. Pontryagin, V.G. Boltyansky, R.V. Gamkrelidze, E.F. Mischenko, Mathematical Theory of Optimal Processes, Nauka, Moskow, 1976, p. 392 (in Russian).
[13] L.I. Anatychuk, V.A. Semenyuk, Optimal Control by Thermoelectric Materials and Devices Properties, Prut, Chernivtsi, 1992, p. 264 (in Russian).
[14] L.I. Anatychuk, L.N. Vikhor, Proceedings of the 14th International Conference on Thermoelectrics, St. Petersburg, 1995, p. 372.
[15] T. Caillat, J.-P. Fleurial, G.J. Snyder, A. Borshchevsky, Proceedings of the 20th International Conference on Thermoelectrics, Beijing, 2001, p. 282.